Arp2/3 promotes junction formation and maintenance in the *Caenorhabditis elegans* intestine by regulating membrane association of apical proteins

Yelena Y. Bernadskaya, Falshruti B. Patel, Hsiao-Ting Hsu, and Martha C. Soto
Department of Pathology and Laboratory Medicine, University of Medicine and Dentistry of New Jersey–Robert Wood Johnson Medical School, Piscataway, NJ 08854

ABSTRACT **It has been proposed that Arp2/3, which promotes nucleation of branched actin, is needed for epithelial junction initiation but is less important as junctions mature. We focus here on how Arp2/3 contributes to the *Caenorhabditis elegans* intestinal epithelium and find important roles for Arp2/3 in the maturation and maintenance of junctions in embryos and adults. Electron microscope studies show that embryos depleted of Arp2/3 form apical actin-rich microvilli and electron-dense apical junctions. However, whereas apical/basal polarity initiates, apical maturation is defective, including decreased apical F-actin enrichment, aberrant lumen morphology, and reduced accumulation of some apical junctional proteins, including DLG-1. Depletion of Arp2/3 in adult animals leads to similar intestinal defects. The DLG-1/AJM-1 apical junction proteins, and the ezrin–radixin–moesin homologue ERM-1, a protein that connects F-actin to membranes, are required along with Arp2/3 for apical F-actin enrichment in embryos, whereas cadherin junction proteins are not. Arp2/3 affects the subcellular distribution of DLG-1 and ERM-1. Loss of Arp2/3 shifts both ERM-1 and DLG-1 from pellet fractions to supernatant fractions, suggesting a role for Arp2/3 in the distribution of membrane-associated proteins. Thus, Arp2/3 is required as junctions mature to maintain apical proteins associated with the correct membranes.**

Monitoring Editor
Alpha Yap
University of Queensland

Received: Nov 1, 2010
Revised: Jun 6, 2011
Accepted: Jun 10, 2011

INTRODUCTION

The actin cytoskeleton contributes to epithelial cell polarity and organization in multiple ways. One essential role for filamentous, or F-actin, is to establish the apical domain of epithelia through its interactions with the adherens junctions. Our understanding of the interaction of actin and the apical junction is currently being revised. Recent studies demonstrate the need for formins and myosin II in the development of the apical actin belt (Smutny and Yap, 2010; Yonemura *et al.*, 2010). The Arp2/3 complex promotes branched actin formation by nucleating new polymers of actin on the sides of existing actin filaments (reviewed in Chhabra and Higgs, 2007). Tissue culture studies show that Arp2/3 is required for cellular protrusions that bring cells together during the establishment of junctions (Yamada and Nelson, 2007). However, these studies propose that Arp2/3 is no longer needed at junctions once they are established. The key molecule believed to link F-actin to the adherens junction is α-catenin. In vitro and tissue culture studies show that dimers of α-catenin are potent inhibitors of actin nucleation by Arp2/3, suggesting an antagonistic relationship between Arp2/3 and α-catenin (Drees *et al.*, 2005; Benjamin *et al.*, 2010). A positive role for Arp2/3 at junctions has been proposed during development of the *Drosophila* notum epithelium, where Arp2/3 and its activator Wiskott–Aldrich syndrome protein (WASP) promote E-cadherin endocytosis at adherens junctions (Leibfried *et al.*, 2008; Georgiou *et al.*, 2008; Fricke *et al.*, 2009). In addition, a study of mammalian metastasis suppressors implicated another Arp2/3 activator, the WAVE/SCAR complex, in adherens junction maintenance, as loss of the WAVE

This article was published online ahead of print in MBoC in Press (http://www.molbiolcell.org/cgi/doi/10.1091/mbc.E10-10-0862) on June 22, 2011.

Address correspondence to: Martha C. Soto (sotomc@umdnj.edu).

Abbreviations used: Arp, actin-related protein; WASP, Wiskott-Aldrich syndrome protein; WAVE/SCAR, WASP family verprolin-homologous/suppressor of cyclic AMP receptor.

component CYFIP led to disruption of E-cadherin distribution at junctions in multiple cancer cell types and in immortalized cells (Silva *et al.*, 2009).

The *Caenorhabditis elegans* apical junction contains two molecularly and functionally distinct junctional complexes—the more apical cadherin/catenin complex (CCC) and, just basal to the CCC, the DLG-1/AJM-1 complex (DAC; reviewed in Labouesse, 2006). The *C. elegans* CCC, including the α-catenin homologue HMP-1, is required for the attachment of actin filaments to adherens junctions (AJs) during the late morphogenetic process of epidermal constriction that leads the embryo to assume its elongated worm shape. However, unlike in *Drosophila* and in vertebrates, loss of the CCC alone does not alter cell polarity, cell adhesion, or the formation of the electron-dense component of the apical junction (Costa *et al.*, 1998; Raich *et al.*, 1999). The DAC components DLG-1 and AJM-1 are also required for epidermal morphogenesis. In contrast to CCC components, loss of DLG-1 disrupts formation of the electron-dense component of the apical junction and results in mild adhesion and polarity defects (Bossinger *et al.*, 2001; Firestein and Rongo, 2001; McMahon *et al.*, 2001). DLG-1 is required for correct AJM-1 localization at AJs (Koppen *et al.*, 2001; McMahon *et al.*, 2001; Segbert *et al.*, 2004). How this second complex connects to the plasma membrane is not well understood, although SAX-7/LICAM, which colocalizes with AJM-1 in the intestine, has been proposed to be the transmembrane component of this junctional complex (Chen *et al.*, 2001). SAX-7 functions redundantly with HMR-1/cadherin during *C. elegans* gastrulation (Grana *et al.*, 2010).

We previously described an essential role for the Arp2/3 complex and its activator, the WAVE/SCAR complex, during the earliest cell movements of embryonic morphogenesis in *C. elegans*. Mutations or depletions by RNA interference (RNAi) of the GTPase CED-10/Rac1, any WAVE/SCAR component, or any Arp2/3 component result in complete loss of epidermal cell shape changes and cell movements. The resulting loss of epidermal cell migration leads to the gut on the exterior (Gex) phenotype first described for WAVE/SCAR complex components GEX-2/Sra1/CYFIP and GEX-3/HEM1/Kette/NAP1 (Patel *et al.*, 2008; Soto *et al.*, 2002). In contrast, strains carrying deletions of WASP, a second Arp2/3 activator, are viable, with a low percentage of embryos defective in morphogenesis (Withee *et al.*, 2004), suggesting that WAVE/SCAR is the major nucleation-promoting factor for Arp2/3 during *C. elegans* development, as has been shown during *Drosophila* development (Zallen *et al.*, 2002).

The *C. elegans* intestine is a beautifully simple organ, consisting of only 20 cells that arise during embryonic development. The 20 individual intestinal cells line up bilaterally and develop into a tube with only two cells per segment for most of its length. The inside surface of the tube has an apical lumen containing actin-rich microvilli, supported by the actin- and intermediate filament–rich terminal web. The cells are connected at apical adherens junctions (Leung *et al.*, 1999). In Gex embryos the intestinal cells are able to form a tube that is initially found in the interior of the cell mass, as in wild type. Only after epidermal enclosure fails late in embryonic development does the intestine become mislocalized to the exterior to produce the Gex terminal phenotype (Patel *et al.*, 2008).

Two protein families have been proposed to recruit actin to membranes in *C. elegans* embryos, ERM (ezrin, radixin, moesin) and WAVE/SCAR. ERM proteins are able to connect F-actin to membranes through their association with membrane lipids, including PIP2 (reviewed in Fehon *et al.*, 2010). *C. elegans* has a single ERM homologue, ERM-1, that is essential for the development of the intestinal lumen. In *erm-1* mutants, the lumen of the intestine forms but is blocked by intestinal cysts (Göbel *et al.*, 2004; van Furden *et al.*, 2004). This is believed to occur due to the requirement for ERM-1 to localize junctional proteins to an apicolateral position after initial apical/basal polarity is established (van Furden *et al.*, 2004). Recruitment of the WAVE/SCAR complex and Arp2/3 to membranes is believed to require membrane-bending F-BAR proteins (Fricke *et al.*, 2009; Giuliani *et al.*, 2009). In *C. elegans*, the ABI-1 subunit of the WAVE/SCAR complex has been shown to bind to the F-BAR protein TOCA-2, and mutations in TOCA-2 lead to Gex-like embryonic lethality and morphogenesis defects. In addition, *toca-2* mutants alter the levels of the junctional protein AJM-1 in the epidermis (Giuliani *et al.*, 2009). In *C. elegans* and *Drosophila* cells the WAVE/SCAR component ABI-1 is recruited to membranes (Fricke *et al.*, 2009; Giuliani *et al.*, 2009), whereas in *C. elegans* and mammalian cells the WAVE complex was shown to affect the accumulation of junctional proteins, including E-cadherin (Giuliani *et al.*, 2009; Silva *et al.*, 2009). This suggested that the role of Arp2/3 at junctions goes beyond forming protrusions to bring two cells together, but rather that it may support junction formation and maintenance.

Here we examined the effects of depleting Arp2/3 on the formation and maintenance of the *C. elegans* intestinal cell junctions in the context of a developing embryo. Intestines developing with reduced Arp2/3 or its WAVE/SCAR activators accumulated less apical F-actin, showed altered lumen morphogenesis, and had decreased accumulation of some apical junction proteins, including DLG-1. To better understand the changes in the intestinal lumen, we investigated whether WAVE/SCAR and Arp2/3 affect ERM-1, the *C. elegans* ERM homologue required for intestinal lumen development (Göbel *et al.*, 2004; van Furden *et al.*, 2004), and found that WAVE/SCAR and ERM-1 regulate each other's protein levels and localization. Subcellular fractionation experiments revealed a requirement for Arp2/3 in order for DLG-1 and ERM-1 to stay associated with specific pellet fractions, suggesting that Arp2/3 regulates the membrane association of proteins that establish and maintain the apical junction. Our experiments depleting Arp2/3 from adults yielded similar results, suggesting that Arp2/3 promotes apical F-actin enrichment and lumen morphogenesis by ensuring that junctional complexes are able to associate with membranes during embryonic development and throughout the life of the organism.

RESULTS

Arp2/3 is required during intestinal morphogenesis in *C. elegans* embryos

The WAVE/SCAR and Arp2/3 actin nucleation complexes of *C. elegans* are required during embryonic development for epidermal cell movements (Soto *et al.*, 2002; Patel *et al.*, 2008). Embryos depleted of WAVE/SCAR or Arp2/3 components exhibit a dramatic loss of morphogenetic movements in the epidermis and changes in other tissues, including the developing intestine. The aberrant location and appearance of the embryonic intestine is one of the defining features of the Gex (gut on the exterior) phenotype, which is caused by mutations and loss of components of the WAVE/SCAR complex (Soto *et al.*, 2002). We therefore wished to analyze which events in intestinal development depend on Arp2/3.

F-actin and WAVE proteins are enriched apically in intestinal cells at the developmental time when the apical lumen of the intestine is forming (Patel *et al.*, 2008). We used a *dlg-1::gfp* transgene (Totong *et al.*, 2007) to monitor the establishment and maintenance of the apical junction in Gex mutants. We found that the initial localization of the apical junction is correct in the absence of GEX components. However, by 380 min after first cleavage (the first cell division), the lumen of *gex* mutants became wider than in comparably staged wild-type embryos, and

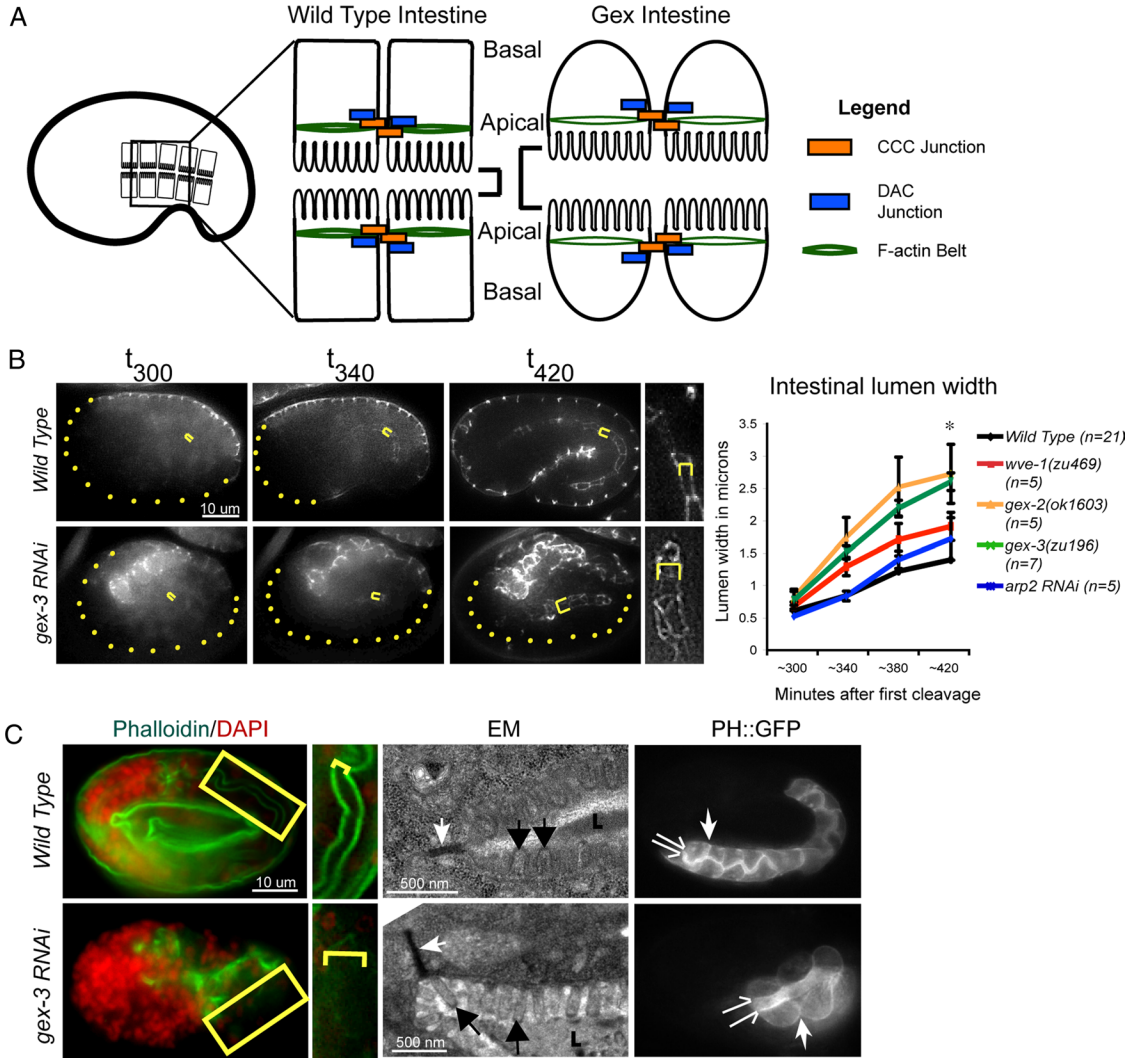

FIGURE 1: Arp2/3 is required during intestinal morphogenesis in *C. elegans* embryos. (A) Wild-type intestinal cells have apical junctions that recruit abundant F-actin; they pack together tightly and form a narrow intestinal lumen. Loss of Arp2/3 or WAVE/SCAR complex genes leads to the Gex, or gut on the exterior, morphogenesis phenotype. Gex intestinal cells recruit less actin at the apical junction; the cells are rounded and form an expanded intestinal lumen. (B) Live imaging to compare the intestinal lumen expansion in wild-type embryos and in embryos depleted of GEX pathway. Embryos are oriented with anterior to the left. The *dlg-1::gfp* transgene (Firestein and Rongo, 2001; Totong *et al.*, 2007) is expressed at the apical junction of epithelial tissues during embryonic development, including the intestine (internal yellow brackets) and the epidermis (expression at the embryo surface). Yellow dots outline parts of the embryo not enclosed by epidermis. Yellow brackets indicate intestinal width. Right, a close-up of the intestine. Image contrast was enhanced equally to highlight intestinal width. Error bars show SEM. Asterisks indicate statistical significance, $p < 0.05$. (C) Left, phalloidin (green) was used to compare apical F-actin levels in wild-type and *gex-3(RNAi)* intestines. The yellow box around part of the intestine is amplified immediately to the right. Yellow brackets indicate intestinal lumen width. Middle, TEM of the intestine in wild-type and *gex-3(RNAi)* embryos. White arrows, apical adherens junctions; black arrows, microvilli; L, intestinal lumen. The white substance inside the lumen is the glycocalix. Right, the *vha-6p::ph::gfp* strain (labeled PH::GFP) was used to visualize cell membranes in wild-type and *gex-3(RNAi)* embryonic intestines. The split arrows illustrate the intestinal lumen width; the white single arrow points to lateral regions.

this expanded width relative to wild type increased over time (Figure 1B). Because this occurred at a time in development when the tissue layers, including the intestine, have the same arrangement in Gex embryos as in wild-type embryos, this change in the intestinal lumen is not likely to be caused by the changes in the external epidermis. Genetic null mutants in *wve-1* never enclose and always show the lumen expansion defect. Partial depletion of *wve-1* by RNAi leads to 50% of embryos that partially or fully enclose before dying. These intermediate-phenotype *wve-1* embryos, even those that enclose, also show the lumen expansion, further supporting that the defect is due to loss of GEX function in the intestine, and not an indirect effect of the epidermal defects (Patel *et al.*, 2008).

Apical F-actin levels decreased by ~30% in *gex-3* embryonic intestinal cells (Figure 1C, left; Figure 3; Patel *et al.*, 2008). To determine whether the drop in apical F-actin levels is due to the loss of microvilli, we performed transmission electron microscopy (TEM) on wild-type and *gex* mutant intestines. Embryos depleted of *gex-3* via RNAi displayed aberrant intestines, but the lumen was covered by microvilli (Figure 1C, middle). The presence of apical microvilli and

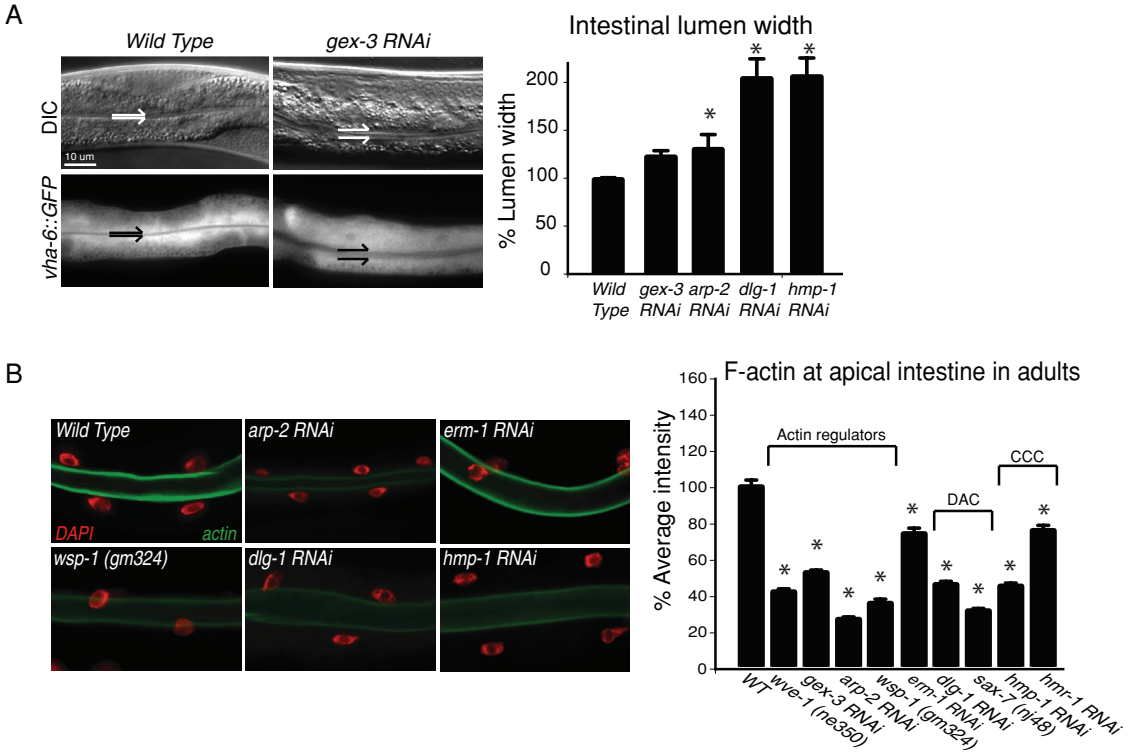

FIGURE 2: Arp2/3 maintains apical organization during postembryonic growth. (A) Adult intestines are shown by differential interference contrast (DIC) (top) and fluorescence optics (bottom). Split arrows indicate intestinal lumen width. Graph shows the lumen width of young adults in wild-type animals and in animals depleted of the WAVE-complex component GEX-3, ARP-2, or apical junction components. A strain that specifically marks the intestinal cells with GFP (*vha-6p::GFP)* facilitated measurement of the lumen width. (B) Postembryonic apical F-actin levels were detected with phalloidin (green) in dissected and fixed intestines. DAPI (red) indicates intestinal nuclei. Graphs: n > 15 adults for each genotype. Error bars show SEM. Asterisks mark statistical significance, $p < 0.05$. Values on the *y*-axis indicate fluorescence intensity in arbitrary units here and throughout the figures.

apical electron-dense adherens junctions (Figure 1C) showed that these cells initiate overall apical/basal polarity. To examine the apical and basolateral morphology of the intestinal cells, we used the PH::GFP transgene expressed under an intestinal promoter (*vha-6p::ph::gfp*; Bae et al., 2009). In wild-type embryos PH::GFP showed tight packing of the intestinal cells at the lateral regions. In embryos depleted of *gex-3* and other WAVE/SCAR components via RNAi, PH::GFP was still enriched at membranes, but the apical lumen was wider and lateral cells packed together more loosely, remaining rounded (Figure 1C, right). These results showed that although apical/basal polarity could initiate in the absence of Arp2/3, the maturation of these intestinal epithelial cells at their apical and lateral regions required Arp2/3.

Arp2/3 regulates intestinal lumen width and apical F-actin accumulation during larval and adult growth

The role of Arp2/3 and its activator, the WAVE/SCAR complex, in embryonic development suggested a role for these actin regulators in the maintenance of tissue polarity. We therefore examined the intestines of adult worms depleted of WAVE/SCAR or Arp2/3 components during larval development. L1 larvae were fed dsRNA to deplete *wve-1*, *gex-3*, *arp-2*, or *wsp-1*, and levels of apically accumulated junctional proteins were monitored after 2 d on RNAi food. Larvae depleted of *arp-2* had additional growth problems; therefore all *arp-2* animals were measured after both 2 and 3 d on RNAi food, and the day 3 results are shown. We detected changes in intestinal lumen width, apical accumulation of junctional proteins, and apical F-actin levels (Figures 2 and 3).

First, we noted that the intestinal lumen became wider when we reduced WAVE/SCAR or Arp2/3 components in adults, just as we saw in embryos. In addition, this lumen expansion also occurred when we reduced the junctional proteins DLG-1 or HMR-1/α-catenin postembryonically (Figure 2A). Second, phalloidin staining of the adult intestine showed a decrease in apical F-actin levels when *wve-1*, *gex-3*, or *arp-2* was removed via mutation or RNAi, similar to the effect observed in embryos (Figure 2B). We conclude that the requirement for Arp2/3 function in the apical intestine begins during embryonic development and continues throughout the life of the worm. In adults the proteins in both junctional complexes—the cadherin/catenin complex, including *hmp-1* and *hmr-1*, and the DLG-1/AJM-1 complex—were required for enriched apical F-actin levels (Figure 2B). These results suggested that Arp2/3 and the two *C. elegans* apical junction complexes work together to regulate the size of the apical lumen and the enrichment of apical F-actin.

Arp2/3 regulates some apical junction components in embryos and adults

We tested whether loss of Arp2/3 and its WAVE regulators affected enrichment of junctional proteins at the apical intestine. Live imaging of DLG-1::GFP accumulation in adult intestines showed that removal of WAVE/SCAR or Arp2/3 components via RNAi resulted in minor overall changes in DLG-1::GFP apical levels and a shift of DLG-1::GFP from the apical region to the cytoplasm, resulting in a lower ratio of apical-to-cytoplasmic fluorescence (Figure 3B). In embryos the apical accumulation of DLG-1 also depended on Arp2/3. In live wild-type embryos the intestine showed increased

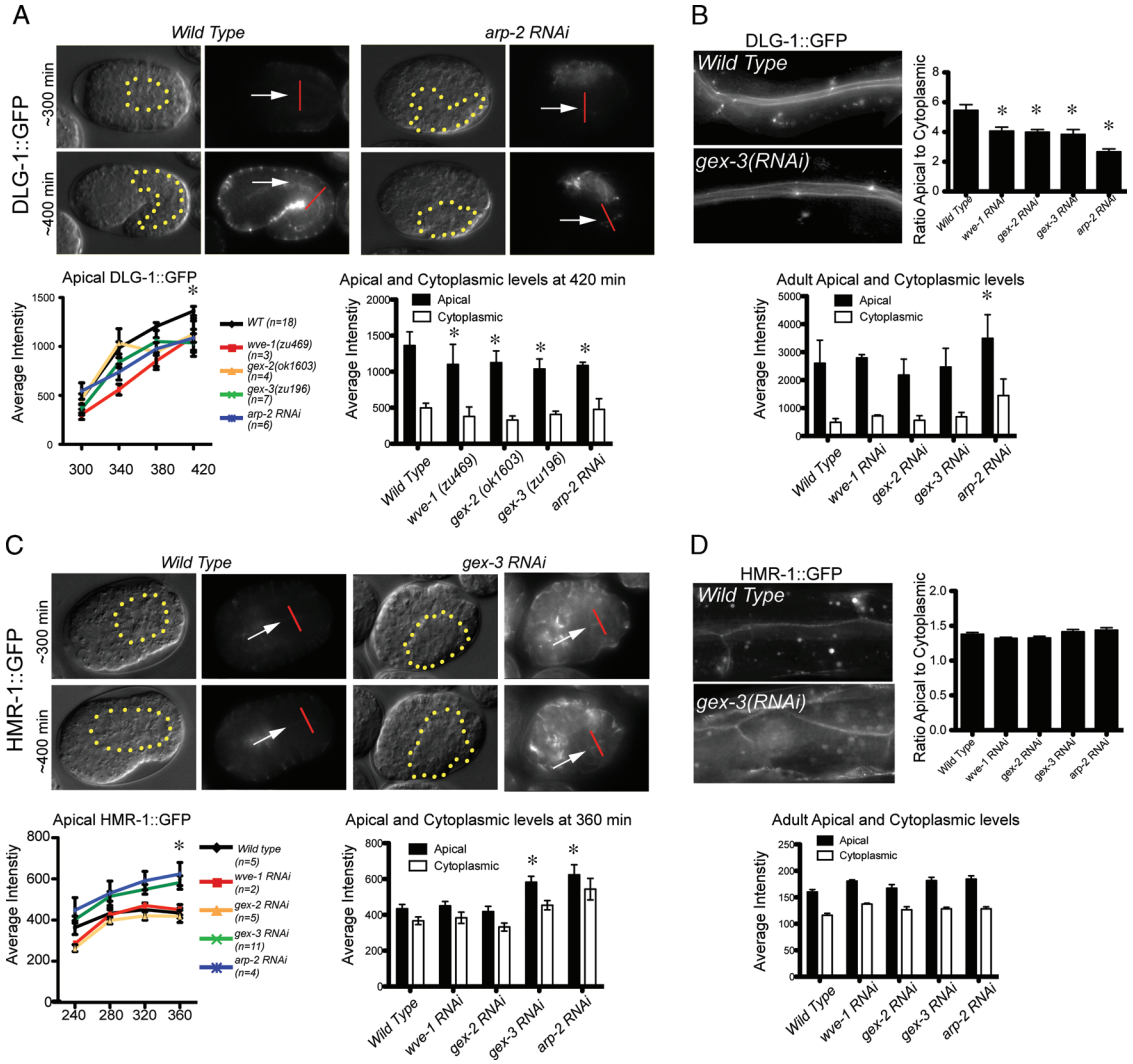

FIGURE 3: Arp2/3 regulates some apical junction components in embryos and adults. (A) Live imaging of DLG-1::GFP during intestinal morphogenesis. The same embryo is shown via DIC optics (left) and fluorescence (right). The levels of DLG-1::GFP were recorded in equally staged wild-type and mutant embryos every 40 min beginning at midembryogenesis. The dotted yellow line indicates the outline of the intestine. White arrows point to the developing apical intestine. The additional signal around the periphery of the embryos is from the DLG-1::GFP expression in the epidermis. The apical intestinal signal was calculated by placing a line (shown in red) across the intestine, and the maximum reading generated using the Line Function of ImageJ was recorded as the apical signal. The cytoplasmic signal was calculated as the average of the signal at the center of the two intestinal cells 2.5 μm on either side of the apical intestine. The graph on the left summarizes the average apical DLG-1::GFP levels in wild-type and Gex embryos; x-axis numbers indicate minutes after first cleavage. The graph on the right shows the average apical and cytoplasmic DLG-1::GFP levels in wild-type and Gex embryos at 420 min after first cleavage. (C) Live imaging of HMR-1::GFP during embryonic intestinal morphogenesis. Labeling, measurements, and graphs were done as in A, except the graph on the right shows the apical and cytoplasmic levels at 360 min after first cleavage. (B, D) DLG-1::GFP and HMR-1::GFP accumulation in adults. Top, the ratio of apical to cytoplasmic. Bottom, apical and cytoplasmic levels of DLG-1::GFP (B) and HMR-1::GFP (D) in the intestines of young adult worms were measured as described for the embryonic intestines. Micrographs show similarly staged worms expressing DLG-1::RFP and HMR-1::GFP. For each genotype $n > 10$ adult worms. Error bars show SEM. Asterisks indicate statistical significance, $p < 0.05$.

apical accumulation of DLG-1::GFP by 340 min after first cleavage, which continued to rise as the intestine formed (Figure 3A). When we reduced WAVE/SCAR and Arp2/3 components from these embryos using RNAi or genetic mutations we noted significantly decreased apical accumulation of DLG-1::GFP by 380 min (Figure 3A). The E-cadherin homologue HMR-1::GFP did not exhibit decreased accumulation at the apical junction in WAVE/SCAR mutants in adults and embryos (Figure 3, C and D). These results show that Arp2/3 is required for the apical enrichment of DLG-1::GFP but not HMR-1/E-cadherin during embryonic and postembryonic growth.

Apical enrichment of F-actin in the embryonic intestine requires the WAVE/SCAR complex, ERM-1, and the DLG-1/AJM-1 junctional complex but not the cadherin/catenin complex

If apical F-actin accumulation in the developing *C. elegans* intestine required the cadherin/catenin complex, then depletion of complex

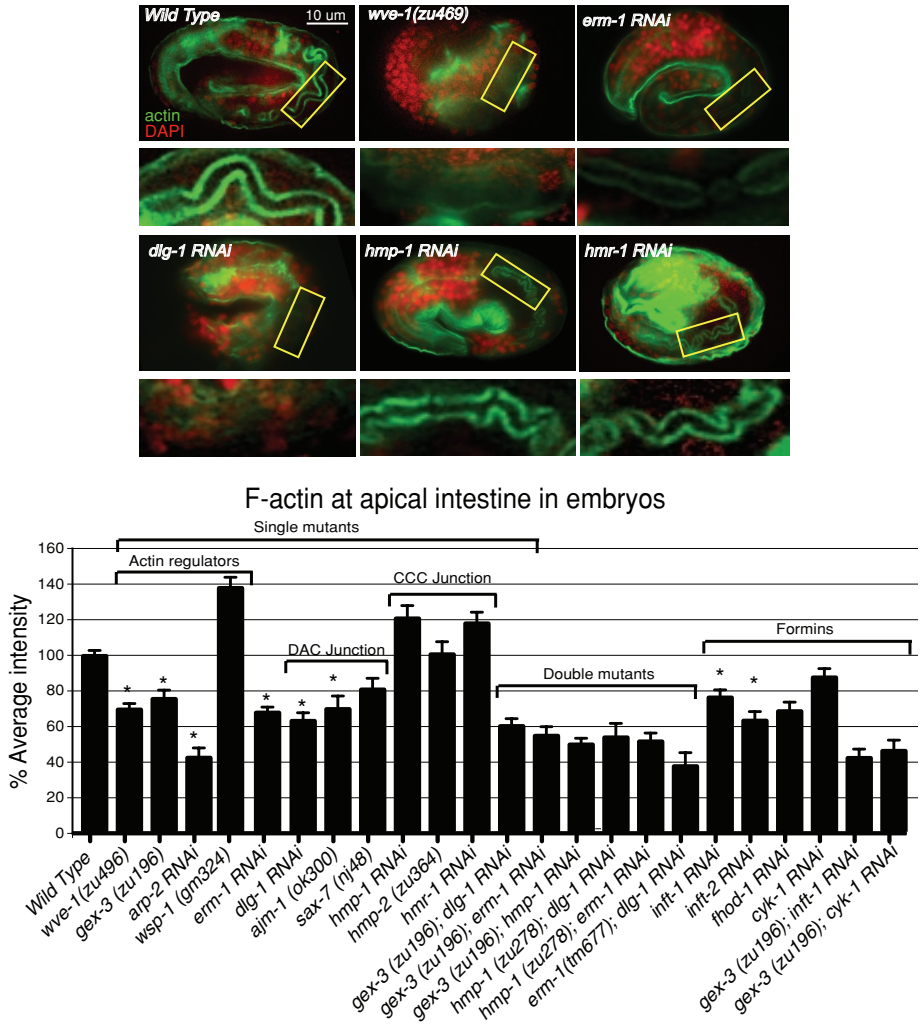

FIGURE 4: Apical enrichment of F-actin in the embryonic intestine requires the WAVE/SCAR complex, ERM-1, and the DLG-1/AJM-1 complex but not the cadherin/catenin complex. Embryos were stained with phalloidin to visualize F-actin (green) accumulation in the apical intestine in wild type and in embryos depleted of candidate regulators of apical morphogenesis. DAPI (red) labels nuclei. The apical region of the intestine (yellow rectangle) is amplified below each micrograph. Embryos at 550 min after first cleavage were compared. Actin regulators, including WAVE/SCAR components *wsp-1*, and *arp-2*, are shown. Double mutants were made by feeding RNAi for one gene to a strain carrying a genetic mutation in a second gene. RNAi effectiveness was verified by phenotypic assays. $n \geq 10$ embryos for each genotype. Error bars show SEM. Asterisks indicate statistical significance, $p < 0.05$.

members should result in a drop of apical F-actin. Surprisingly, phalloidin staining showed that F-actin levels were not significantly lowered by the loss of *hmp-1/α-catenin* or the loss of other components of the cadherin/catenin complex: *hmp-2/β-catenin* and *hmr-1/cadherin* (Figure 4). We conclude that the cadherin/catenin complex is not required for F-actin assembly in the developing *C. elegans* intestinal apical junction.

If the proteins of the second apical junction complex, the DLG-1/AJM-1 complex, are recruiting actin to the apical junction, we would expect loss of DLG-1 or AJM-1 to affect apical F-actin levels. Phalloidin signal at the apical intestine dropped by ~35% in *dlg-1* RNAi embryos and by ~30% in *ajm-1* RNAi embryos (Figure 4). This is comparable to the drop we observed when we reduced WAVE/SCAR components (Figure 4; Patel *et al.*, 2008). We further tested the proposed transmembrane component, SAX-7, using genetic putative null mutations. We failed to detect a significant drop in apical F-actin using the *sax-7 nj48*, *yk146*, and *ok1244* alleles. Furthermore, loss of *sax-7* did not affect the junctional accumulation of AJM-1 or DLG-1::GFP (unpublished data). These results do not support a role for SAX-7 to be the transmembrane protein that localizes DLG-1 and AJM-1 at the membrane. We propose that when the junctions first form, the DLG-1/AJM-1 complex is the main regulator of F-actin through an unidentified actin-binding protein but that in later development and growth the cadherin/catenin complex takes up its expected role to regulate the apical belt actin (Figure 2B). Therefore the DLG-1/AJM-1 complex appears to regulate apical F-actin continuously in the intestine, from embryogenesis to adult growth.

Loss of the *C. elegans* ezrin–radixin–moesin homologue ERM-1 is reported to reduce apical F-actin in the embryonic intestine (Göbel *et al.*, 2004; van Furden *et al.*, 2004). We found that loss of ERM-1 led to a 30% drop in apical actin, similar to the loss of WAVE/SCAR components or loss of DLG-1/AJM-1 components. The effect was apparent in early embryos (240 min; unpublished data), which did not have established apical junctions, as well as in midembryogenesis ERM-1 embryos (440 min and later) that were establishing the junctions (Figure 4). This showed that, similar to the WAVE and DLG-1 complexes, ERM-1 is required for the early recruitment of apical F-actin in the developing intestine.

Genetic evidence that WAVE/SCAR components work with the DLG-1/AJM-1 components and ERM-1 for apical actin enrichment

We used genetic double-mutant analysis to test whether WAVE/SCAR components and ERM-1 act with either the DLG-1/AJM-1 junction, with the cadherin/catenin junction, or with both. Double mutants in the same pathway should show similar effects on apical F-actin, whereas mutants in two parallel pathways may show additive results. ERM-1 had previously been proposed to act in parallel to the cadherin/catenin complex based on the junctional protein accumulation (van Furden *et al.*, 2004). We measured the effects of these mutations on apical F-actin accumulation at the 550-min stage. The cadherin/catenin complex did not affect actin accumulation at this stage, whereas the DLG-1/AJM-1 complex did, as did loss of WAVE complex or of ERM-1. Double mutants showed that loss of *erm-1* did not cause additional loss of apical F-actin in double mutants with WAVE complex component *wve-1* or *gex-3* (Figure 4). Likewise the loss of both *gex-3* and *dlg-1* led to a similar decrease in apical F-actin as either single mutant. The loss of both *hmp-1/α-catenin* and *dlg-1* led to a similar drop in apical F-actin levels as the loss of *dlg-1* (Figure 4). These results suggest that ERM-1, the WAVE complex, and the DLG-1 complex work together to recruit apical actin, since the double mutants lead to the same decrease in

apical F-actin levels as any of the single mutants. The cadherin complex did not play a role in this embryonic recruitment of apical F-actin, even when the other components were missing, suggesting that redundancy is not hiding the role of the cadherin complex. We note that none of the double deletions and knockdowns led to complete loss of apical F-actin. The remaining apical F-actin may be present in microvilli, as shown by EM of single mutants (Figure 1B; Göbel *et al.*, 2004). This remaining F-actin may be nucleated by formins. *C. elegans* has seven formin-like proteins. Removal of individual formins led to variable decreases in apical phalloidin levels. Double mutants formed by reducing the formins *inft-1* or *cyk-1* via RNAi in *gex-3* embryos led to lower levels of phalloidin than in any of the single mutants (Figure 4). This suggests that all of the actin nucleators—those that promote linear actin and those that promote branched actin—contribute to the apical actin accumulation in the developing intestine.

The WAVE/SCAR complex regulates intestinal morphogenesis through ERM-1

The single *C. elegans* ERM homologue ERM-1 is essential for the development of the intestinal lumen. Loss of ERM-1 reduced apical F-actin levels in the early embryonic intestine as severely as did loss of WAVE/SCAR components or Arp2/3 (Figure 4).

We therefore investigated whether WAVE/SCAR proteins and ERM-1 proteins work together at the apical junction by testing where they localize relative to each other, how similar or different their effects are at the apical junction, and whether they affect each other's localization and levels.

The WAVE/SCAR complex localizes between the apical ERM-1 domain and the apical junction. We performed double-label experiments to determine the localization of the WAVE complex relative to ERM-1 and to the apical junctions at the time of junctional establishment, between 280 and 450 min after first cleavage. Embryos doubly labeled with antibodies to ERM-1 and to green fluorescent protein (GFP) to visualize DLG-1::GFP showed that ERM-1 and the junctional protein DLG-1 overlapped initially at the apical intestine as previously described (van Furden *et al.*, 2004; and unpublished data), but ERM-1 localized apically to DLG-1 by 440 min (Figure 5A). ERM-1 also localized apically to the CCC complex component HMR-1/E-cadherin by 440 min (Figure 5A). Embryos doubly labeled with an antibody to the junctional protein AJM-1 (MH27; Francis and Waterston, 1991; Koppen *et al.*, 2001) and an antibody to GFP to visualize GFP::GEX-3 showed that GFP::GEX-3 was enriched apically to AJM-1 by 460 min (Figure 5A). Embryos doubly labeled with antibody to ERM-1 and an antibody to GFP to visualize GFP::GEX-3 showed that WAVE complex components were enriched basally to ERM-1 by 440 min (600 min shown; Figure 5A). Therefore in these cells the WAVE/SCAR components are enriched apically between ERM-1 and the apical junctions as the junctions are assuming their apicolateral position.

Comparison of Erm and Gex phenotypes in lumen morphology and DLG-1 recruitment. To compare the role of ERM-1 at junctions with the role of WAVE/SCAR, we first compared their effects on the intestinal lumen width. The *gex-3(zu196);dlg-1::gfp* embryos showed progressive expansion of the apical lumen, whereas the *erm-1(RNAi);dlg-1::gfp* embryos showed the opposite phenotype—a narrower intestinal lumen (Figure 5B). To test whether the lumen expansion in Gex mutants depends on ERM-1, we depleted *erm-1* from *gex-3* mutant embryos. The *gex-3(zu196);erm-1(RNAi);dlg-1::gfp* embryos showed an expansion of the intestinal lumen close to that of wild type (Figure 5B). This suggested that GEX-3 requires ERM-1 to affect the width of the lumen.

Although loss of *gex-3* led to lower apical DLG-1::GFP accumulation (Figures 3A and 5B), loss of ERM-1 did not significantly affect apical accumulation of DLG-1::GFP (Figure 5B), consistent with reports that DLG-1 can accumulate without ERM-1 (van Furden *et al.*, 2004). However, if both *erm-1* and *gex-3* were removed, even less DLG-1::GFP accumulated at the apical intestine than when *gex-3* alone was removed (Figure 5B). Likewise, the levels of phalloidin dropped by a similar amount (~30%) when both *erm-1* and *gex-3* were removed (Figure 4; summarized in Figure 5B). In contrast, the levels of HMR-1::GFP were not significantly altered by the loss of *gex-3* or *erm-1* or in the double mutant (Figure 5B). This showed that both ERM-1 and GEX-3 were contributing to the apical recruitment of F-actin and of some apical junction proteins, but the apical F-actin levels correlated with the levels of DLG-1, not of cadherin/HMR-1.

WAVE and ERM-1 effects on each other's protein levels

ERM-1 regulates the apical accumulation of GFP::GEX-3 and the total protein levels of WVE-1. To test whether loss of ERM-1 affects the normal distribution of WAVE complex components, we performed antibody staining to GFP and to AJM-1 on embryos carrying the rescuing *gfp::gex-3* transgene and found that apical accumulation of GFP::GEX-3 required ERM-1. In 10 of 10 embryos we saw that the apical junction protein AJM-1 accumulated at its normal apical location when ERM-1 was removed by RNAi, but GFP::GEX-3 did not become enriched at the apical intestine, and the overall levels seemed reduced (Figure 5A, rightmost). We measured the levels of WVE-1 in lysates depleted of ERM-1 and detected a decrease of at least 50% (Figure 5C). Because loss of any component of the WAVE complex reduces the levels of all complex members (Patel *et al.*, 2008), these results suggested that less WAVE complex can accumulate apically in embryos depleted of ERM-1. This could be due to the overall drop in WAVE levels or to a requirement for ERM-1 to help the WAVE complex accumulate at the apical membrane.

Apr2/3 regulates the accumulation of apical ERM-1 and total protein levels of ERM-1. To test whether loss of Arp2/3 affects the normal distribution of ERM-1, we measured the apical accumulation of ERM-1::GFP in the presence and absence of the Arp2/3 regulator *gex-3* in live embryos (Figure 5C). Wild-type embryos at 420 min showed similar levels of DLG-1::RFP and ERM-1::GFP at the apical surface of the intestine. Although *gex-3(RNAi)* embryos at 420 min showed slightly decreased apical accumulation of DLG-1::RFP compared with wild-type embryos, the mutants accumulated 50% more apical ERM-1::GFP than does wild type (Figure 5C). This result supports a role for Apr2/3 down-regulating the levels of ERM-1.

We measured the levels of ERM-1 in lysates depleted of *wve-1*, *gex-2*, *gex-3*, or *arp-2* and detected an increase of greater than 10-fold in all of the depleted lysates (Figure 5C). Therefore WAVE/SCAR and ERM-1 proteins regulate each other's protein levels, with ERM-1 contributing to WVE-1 levels and WVE-1 in contrast limiting ERM-1 levels. This can be seen in the total levels of the relative proteins and in their accumulation in live embryos. These results raised the question of whether the apical changes detected by live imaging reflected changes in the ability of these proteins to associate with membranes, including the apical membrane.

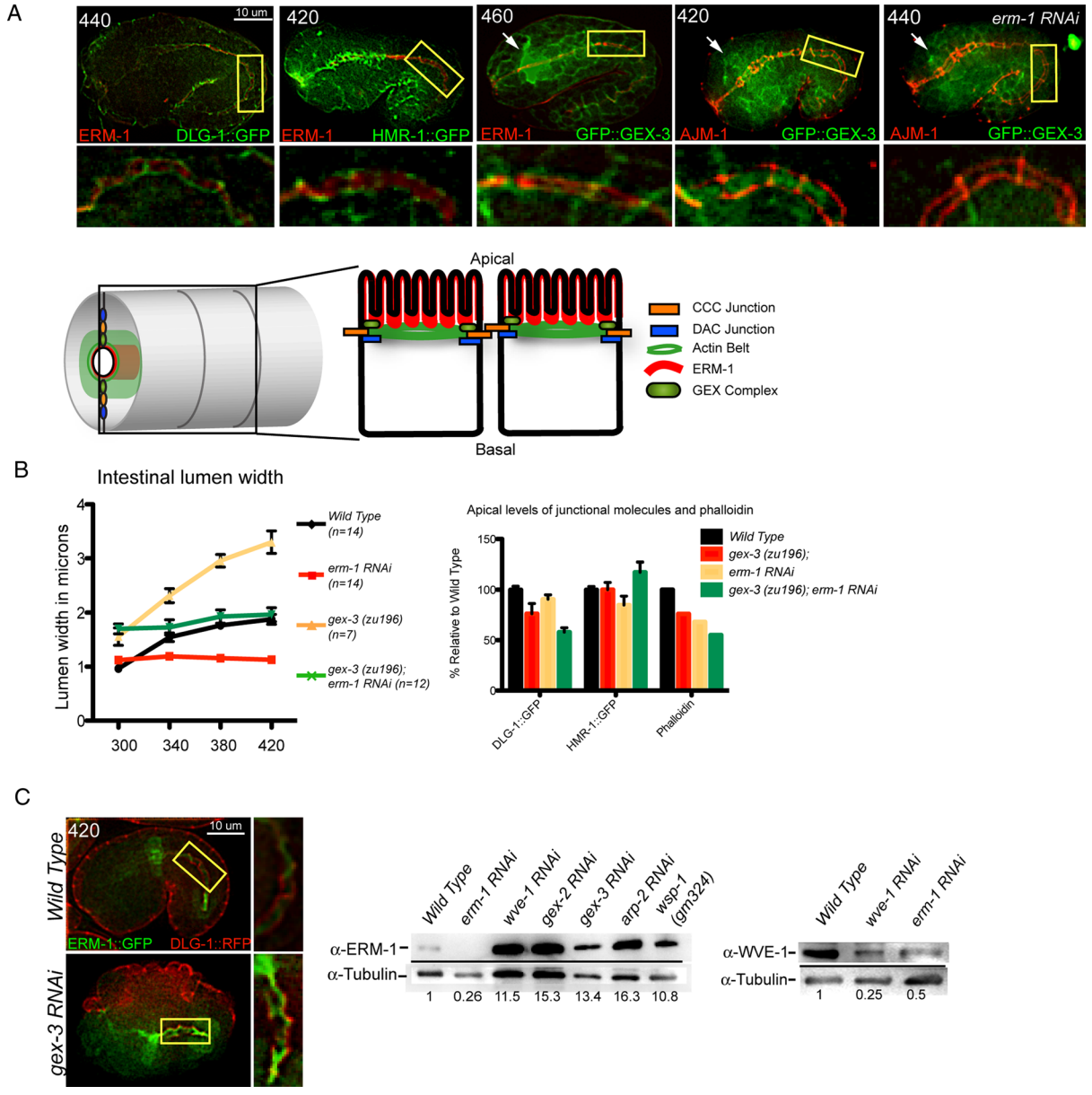

FIGURE 5: The WAVE/SCAR complex regulates intestinal morphogenesis through ERM-1. (A) Localization of WAVE proteins relative to ERM-1 and the apical junction. Fixed embryos doubly labeled with antibodies to ERM-1 (Hadwiger *et al.*, 2010), AJM-1 (MH27) (Francis and Waterston, 1991; Koppen *et al.*, 2001), and GFP (ab6556, Abcam) to visualize DLG-1::GFP (Totong *et al.*, 2007) and a GFP::GEX-3–rescuing transgene (Soto *et al.*, 2002). Age of embryos in minutes after first cleavage is indicated at upper left. All embryos are in a wild-type genetic background, except for the embryo at the right, which was depleted of ERM-1 via RNAi. White arrows point to the developing nerve ring, which in wild-type embryos has high GFP::GEX-3 expression. Image contrast was enhanced equally to better illustrate the subcellular localization. Section of the intestine in the yellow rectangle is amplified below the micrograph. The bright spot on the upper right corner of the rightmost embryo is nonspecific signal, visible in all channels. The model shows the location of ERM-1 (red) relative to WAVE/SCAR (light green) and the DAC junction (blue). (B) Comparison of the effects of WAVE and/or ERM-1 loss on apical intestine development. Left, embryos carrying the *dlg-1::gfp* transgene were used to monitor the width of the intestinal lumen over time in wild-type, *erm-1(RNAi)*, *gex-3(zu196)*, and *gex-3(zu196);erm-1* (RNAi) strains. Right, comparison of changes in the apical DLG-1::GFP, HMR-1::GFP, and phalloidin levels in *erm-1(RNAi)*, *gex-3(zu196)*, and *gex-3(zu196);erm-1* (RNAi) strains. Measurements of apical DLG-1::GFP and HMR-1::GFP were taken as described in Figure 3. Phalloidin data are from Figure 4. (C) WAVE and ERM-1 effects on each other's protein levels. Live embryos carrying two transgenes, DLG-1::RFP and ERM-1::GFP, imaged with wild type and reduced (*gex-3 RNAi*) WAVE complex. Magnified image of the intestine in the merged image is shown to the right. Image contrast was enhanced equally to better illustrate the localization, but quantitation was performed on raw images. Western blot analysis of ERM-1 levels in lysates depleted of branched actin regulators (middle) and of WVE-1 levels in lysates depleted of ERM-1 (right). Numbers below the blots show fold increase over wild type as normalized to tubulin and represent the average of two independent sets of lysates and three blots (ERM-1 Western) and three independent sets of lysates and seven blots (WVE-1 Western). Error bars show SEM. Asterisks mark statistical significance, $p < 0.05$.

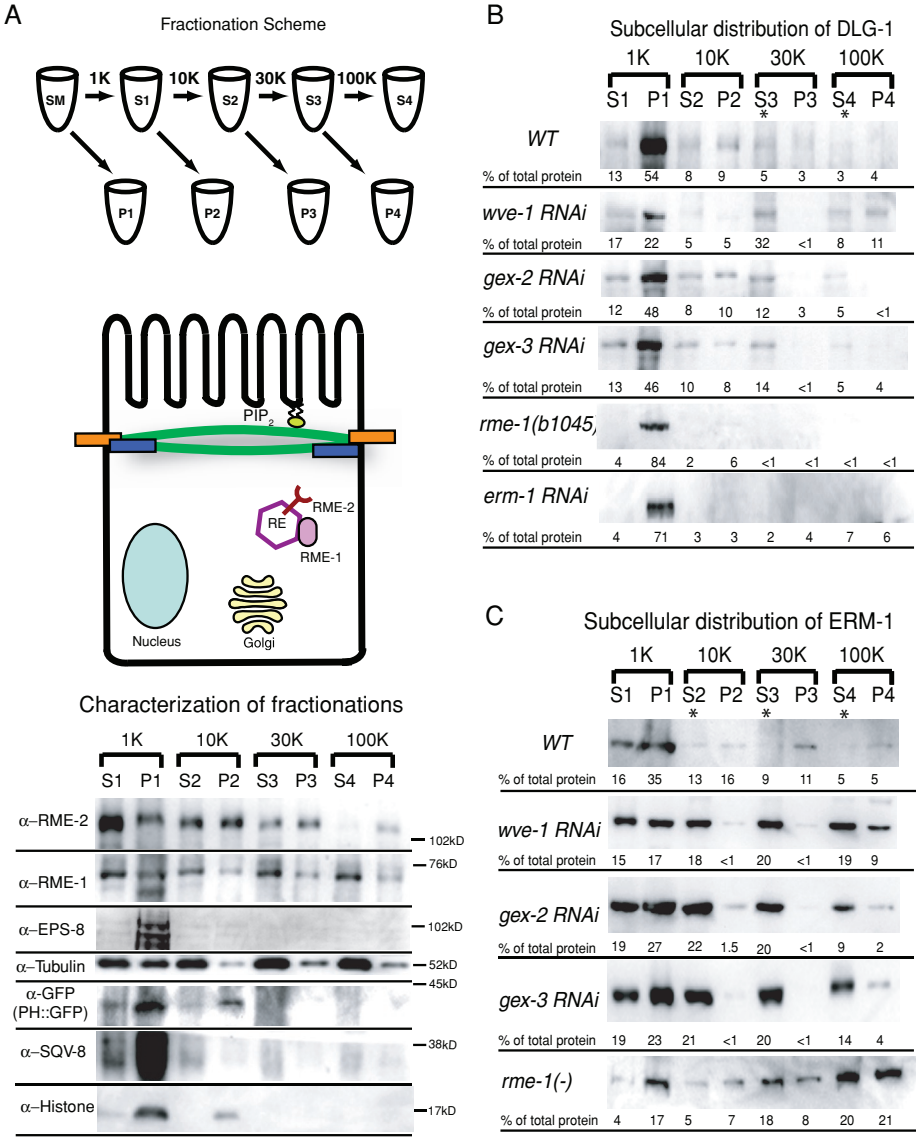

FIGURE 6: Subcellular distribution of ERM-1 and DLG-1 depends on the WAVE complex. (A) Fractionation scheme and characterization of the supernatant and pellet fractions (see *Materials and Methods* for details). Pellets were resuspended so that they matched the volume of their partner supernatant fraction, then equal volumes of each S and P fraction were loaded so that relative amounts of each protein in the S vs. P fraction could be compared. Antibodies to specific subcellular components were used to characterize the fractions. RE, recycling endosome; SM, starting material. (B) Subcellular distribution of DLG-1 visualized with an antibody to GFP in wild-type, *wve-1*, *gex-2*, and *gex-3 RNAi* lysates and with an antibody to endogenous DLG-1 (Hadwiger *et al.*, 2010) in *rme-1(b1045)* mutant and *erm-1 RNAi* lysates. (C) Subcellular distribution of ERM-1 visualized with an antibody to endogenous ERM-1 in wild-type and mutant lysates. Asterisks indicate a shift of protein from the pellet to the supernatant fraction in mutant lysates. The numbers below each band represent the relative percentage of total protein found in each fraction and are the average data from at least three Western blots representing at least two separate fractionation experiments for each genotype.

Subcellular fractionations reveal that Arp2/3 regulates DLG-1 and ERM-1 distribution at cellular membranes

The changes in the accumulation of DLG-1 and ERM-1 at the apical intestine of Gex embryos could reflect changes in how much of these junctional proteins are membrane associated or changes in how much of these proteins are cytoplasmic but enriched near the apical membrane. To distinguish between these two possibilities, we pursued subcellular fractionations of *C. elegans* lysates. There are few published protocols for subcellular fractionation in *C. elegans*, so we developed a protocol based on the published *Saccharomyces cerevisiae* and mammalian fractionation protocols (Figure 6A; *Materials and Methods*). We then used antibodies to characterize the supernatant (S) and pellet (P) fractions that we obtained after separating the fractions with increasing rotation speed and duration (Figure 6A). Antibodies to DNA-associated histone H3 (Abcam Ab1791) bound mainly to the P1 fraction, and a smaller proportion bound to the P2 fraction, which showed that the fractionation conditions were gentle enough to not lyse nuclei. The presence of histone H3 in the P2 fraction likely reflected mitochondrial DNA, which also contains H3 histones (Zanin *et al.*, 2010). Antibodies to the Golgi component SQV-8 (Audhya *et al.*, 2007) bound mainly to the P1 fraction, which indicated that the P1 fraction was enriched in large organelles. PLC-δ-PH::GFP (abbreviated PH::GFP) binds to phosphatidylinositol bisphosphate (PIP_2) and is therefore enriched at the plasma membrane (Stauffer *et al.*, 1998; Varnai and Balla, 1998; Bae *et al.*, 2009). Antibodies to GFP showed that PH::GFP was enriched in P1 and P2, suggesting that these fractions contained a significant part of the plasma membrane. Vertebrate intestinal brush border fractions, which contain junctional complexes, can be isolated by low-speed centrifugation of whole-cell homogenates (Schafer *et al.*, 1992). Therefore P1 may contain the apical plasma membrane associated with microvilli and the apical junction. To test this idea, we determined the distribution of EPS-8, a protein that localizes to apical cellular structures, including the intestinal microvilli, in *C. elegans* (Croce *et al.*, 2004; Ding *et al.*, 2008). Antibodies to EPS-8 (Croce *et al.*, 2004) bound mainly to the P1 fraction. Antibodies to tubulin showed increasing enrichment in the supernatant fractions. A faint band of tubulin was always seen in the high-speed pellet, P4. This is likely the small pool of membrane-associated tubulin that has been reported in other organisms (Allen and Wolf, 1979; Nishikawa and Kitamura, 1984; Farah *et al.*, 2005).

DLG-1 and ERM-1 are membrane-associated rather than transmembrane proteins. We therefore characterized the subcellular distribution of membrane-associated proteins as compared with transmembrane proteins in our fractions (Figure 6A). Antibodies to the transmembrane protein RME-2, the *C. elegans* yolk receptor that is most abundantly found at recycling endosomes (Grant and Hirsh, 1999), bound strongly to the pellet fractions P2, P3, and P4, with the highest amount in the P2, and only faintly to the S4 fraction. Therefore the pellet fractions appeared enriched in transmembrane proteins. In contrast, antibodies to the membrane-associated recycling endosome protein RME-1 (Grant *et al.*, 2001) became

enriched in the supernatant fractions S2, S3, and S4. However, a small but significant percentage of RME-1 also associated with the pellet fractions, including P4. This suggested that under these fractionation conditions we were able to detect the membrane association of proteins and could distinguish these proteins from transmembrane proteins. With these fractionation conditions, we next analyzed the subcellular distribution of ERM-1 and DLG-1.

Subcellular fractionation of embryos suggested that in wild-type DLG-1 was enriched in membrane fractions (Figure 6B) but that loss of Apr2/3 or its activators shifted DLG-1 from the plasma membrane to other subcellular compartments. Lysates from wild-type embryos showed that most DLG-1::GFP was enriched in P1 pellet (54%, of total protein), with significant amounts of DLG-1::GFP in the P2 and P4 pellets (9 and 4% of total protein each). This profile was most similar to that of PLC-δ-PH::GFP, which was enriched in P1 and P2 pellets (Figure 6A). When we reduced WAVE/SCAR components from these embryos via RNAi, we noted that the P1 pellet still contained most of the DLG-1::GFP, but now a significant percentage of DLG-1::GFP was found in the remaining higher-speed S and P fractions. In particular, we measured an increase in the percentage of the total lysates contributing to the S3 fraction, from 5% of the total lysate in wild type to 32, 12, and 14%, respectively, in lysates depleted of *wve-1*, *gex-2*, *or gex-3* (Figure 6B). The decreased accumulation of DLG-1::GFP at the apical junctions in live embryos (Figure 3A) may reflect a shift to a different subcellular domain. The S3 fraction is enriched for RME-1, a membrane-associated component of the basolateral recycling endosomes (Grant *et al.*, 2001; Chen *et al.*, 2006). Therefore, the shift to the S3 fraction could reflect a shift of DLG-1 away from the plasma membrane and to recycling endosomes. To test this idea, we made lysates from animals with a null mutation in the recycling endosome protein RME-1. Using an antibody to endogenous DLG-1 (Hadwiger *et al.*, 2010), we found that there was less DLG-1 in the S3 fraction compared with wild type, whereas the amount of DLG-1 in P1 increased by at least 50% compared with wild type. Because loss of RME-1 results in decreased transport of some proteins from recycling endosomes to the plasma membrane (Grant *et al.*, 2001), this suggested that DLG-1 localization depends on trafficking proteins, that DLG-1 requires the RME-1 pathway for proper localization, and that RME-1 and Arp2/3 have different roles regulating the plasma membrane association of DLG-1. Overall, these fractionation results suggest that Arp2/3 and a regulator of recycling endosomes maintain the apical junction protein DLG-1 in its correct membrane compartment.

To determine the distribution of ERM-1 in wild-type and mutant animals, we probed the fractionated lysates with an antibody to endogenous ERM-1 (Hadwiger *et al.*, 2010) and found that it bound mainly to the P1 low-speed pellet, as would be expected for a protein closely associated with the apical plasma membrane. Depleting WAVE/SCAR component *wve-1*, *gex-2*, or *gex-3* led to a shift of ERM-1 into all of the supernatant fractions, as well as increased ERM-1 levels in the higher -speed fractions (Figure 6C). The substantial shift to the S3 and S4 fractions may indicate that there are increased ERM-1 levels, for example, at recycling endosomes. To test this idea, we used lysates depleted of the recycling endosome protein RME-1 and found increased ERM-1 in the S3 and S4 fractions but an overall shift back to pellet fractions, including P4. Therefore, another membrane-associated protein important for apical intestine development requires Arp2/3 regulators and a regulator of recycling endosomes for its subcellular distribution.

DISCUSSION

Arp2/3-dependent actin nucleation is needed to form protrusions for cell migrations, but in a polarized cell Arp2/3 carries out additional functions to maintain the integrity of apical junctions. In *C. elegans* animals with properly formed junctions, depletion of Arp2/3 or its nucleation-promoting factor WAVE/SCAR led to changes at the apical junctions in both larvae and adults. These changes match those caused by removal of actin nucleators in developing embryos. Loss of Arp2/3 in the self-assembling tubular intestine of *C. elegans* does not disturb the establishment of apical/basal regions of these cells. The results shown here demonstrate that the maturation of the apical domains requires Arp2/3. In the absence of Arp2/3 or its WAVE/SCAR regulators, the developing embryonic intestine shows decreased apical enrichment of F-actin and altered distribution of apical junction molecules. We show here that 1) the cadherin/catenin complex is not the sole regulator of apical F-actin, as loss of the DLG-1/AJM-1 complex has a greater effect on apical F-actin in the embryonic intestine; 2) Arp2/3 supports the DLG-1/AJM-1 complex to maintain the apical compartment in embryos and larvae; and 3) Two distinct types of proteins, Arp2/3 and ERM-1, promote F-actin enrichment at apical epithelia and regulate the membrane association and distribution of the apical junction protein DLG-1.

These studies connect two complexes that are associated with F-actin at membranes in the development of the apical junction. ERM-1 is needed to exclude junctional proteins, including DLG-1, from the apical region so that these proteins acquire an apicolateral location (van Furden *et al.*, 2004). We show that Arp2/3 contributes to this process by regulating the apical accumulation and total levels of ERM-1. In the absence of WAVE/SCAR, ERM-1 levels are elevated at the apical intestine, whereas DLG-1 levels drop. However, the relationship of WAVE/SCAR and ERM-1 is not simply antagonistic. Both actin-associated proteins contribute to apical F-actin accumulation in the developing intestine, and both are needed for apical accumulation of DLG-1 at the apical junction. This suggests a developmental model, elaborated below and in Figure 7, for how these two actin-associated proteins may work together to support the maturation of junctions in the developing intestine.

Developmental model for how Arp2/3 supports epithelial polarization

As epithelial cells polarize, actin is enriched at one end of the cell. ERM proteins are able to interpret polarity signals and to connect cortical F-actin to the plasma membrane (Fehon *et al.*, 2010). In the developing *C. elegans* intestine this apical domain is initially rich in junctional proteins, including DLG-1. However, as the cells are further polarized, the junctional proteins are repositioned to apicolateral domains of the plasma membrane, and this localization depends on ERMs (van Furden *et al.*, 2004). How ERM-1 accomplishes this is not known. As these events are occurring, WAVE proteins are also accumulating at the apical region of the cell (Patel *et al.*, 2008) and eventually mark the boundary between ERM-1 and the apical junction (Figure 5A). Enrichment of WAVE proteins at the apical membrane requires ERM-1 (Figure 5A). The fact that WAVE proteins in the *C. elegans* intestine are needed only after epithelial polarization has begun is illustrated by the fact that several proteins that establish apical/basal polarity, such as PAR-3 and the Scribble homologue LET-413, are able to assemble properly in the absence of WAVE/SCAR (unpublished data), and EM studies show that adherens junctions form (Figure 1C). When WAVE complex proteins are missing, the earliest defects we observed were in the membrane accumulation and retention of a subset of the apical junction proteins, in particular DLG-1. Subcellular fractionations support the idea that Arp2/3

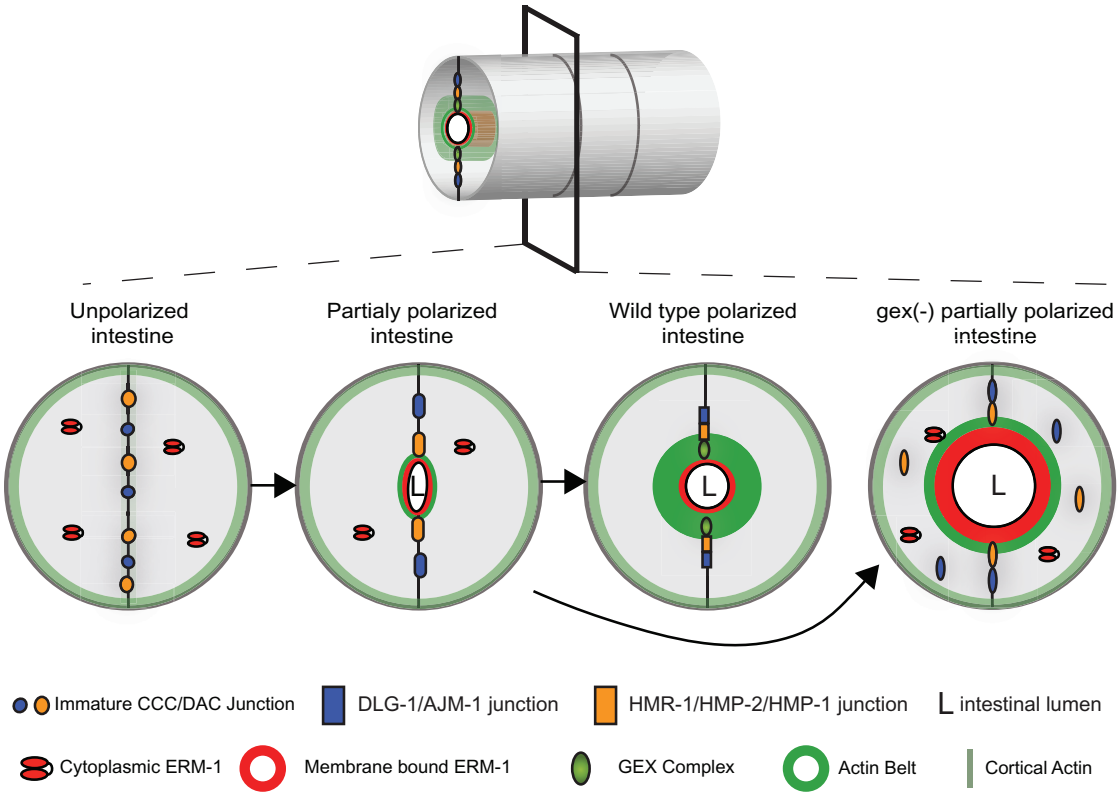

FIGURE 7: A developmental model for the role of Arp2/3 and ERM-1 in apical junction formation during development. Cross–sections of the intestinal tube are shown in developing wild-type and Gex embryos. Polarization of intestinal cells requires the assembly of the apical domain, including apical localization of the junctions, ERM-1, the WAVE/SCAR complex, and F-actin. ERM-1 helps to establish the apical region by binding to cortical F-actin before the apical junctions have fully formed, by localizing WAVE/SCAR apically, and by repositioning the apical junction proteins apicolaterally. When Arp2/3 is present the correct levels of ERM-1 accumulate at the apical plasma membrane, and junctional proteins can accumulate at their correct apicolateral locations. In the absence of Arp2/3 or its activator, the WAVE/SCAR complex, ERM-1 levels are highly elevated. The elevated ERM-1 may displace junctional proteins from the apical domain, leading to decreased junctional proteins at the membrane, less apical F-actin, and an expanded lumen width. Taken together, these defects result in a cell that is only partially polarized.

regulates the membrane association of these junctional proteins. The consequences of reducing the amounts of junctional proteins from the apical junction are a reduction in apical actin (Figures 1, 2, and 4) and an expansion of the lumen width (Figure 1, 2, and 5).

What may branched actin be contributing to apical junctions during development?

Arp2/3-dependent actin nucleation may be contributing to apical F-actin establishment and retention in two ways: 1) through a structural role and 2) through a regulatory role.

Structural role. Branched actin nucleated by Arp2/3 could provide stiffness that could set the boundaries of the apical versus apicolateral domain of the plasma membrane. This difference in stiffness could limit the region where ERM-1 acts and could support the membrane recruitment of apical junction proteins. In addition, activated ERM proteins have been shown to provide stiffness to membranes (Manno *et al.*, 2005; Cheshire *et al.*, 2008; Kunda *et al.*, 2008). The decreased lumen expansion and collapsed lumen seen in *erm-1* mutants may indicate that ERM-1 is needed to provide stiffness during lumen formation. The increased lumen expansion and increased ERM-1 levels seen in *gex* mutants may indicate that WAVE/SCAR proteins prevent excessive apical stiffness and lumen expansion by down-regulating ERM-1. Phospho-specific antibodies to activated ERM-1 could be used to test this model.

Regulatory role. Studies in *C. elegans*, *Drosophila*, and mammalian tissues have proposed a role for Arp2/3 in the trafficking of junctional proteins, for example, of E-cadherin, at the apical junction. The exact step in trafficking that is altered by the loss of Arp2/3 is not known, but it has been proposed that scission of membrane tubules undergoing endocytosis is one role for Arp2/3 (Georgiou *et al.*, 2008; Leibfried *et al.*, 2008; Fricke *et al.*, 2009). The results shown here support a trafficking role for Arp2/3 distinct from the role of recycling endosome proteins like the EH domain protein RME-1: Arp2/3 may help transport membrane-associated molecules like ERM-1 and DLG-1 from the plasma membrane to recycling endosomes. These studies suggest that correct subcellular distributions of ERM-1 and DLG-1 are essential for maintenance of intestinal lumen morphology and of the apical junction. A trafficking role for ERM-1 is well documented, including for the transition of early endosomes to late endosomes in conjunction with the homotypic fusion and vacuole protein sorting protein complex (Chirivino *et al.*, 2011). Therefore a change in the subcellular localization of ERM-1 could affect proteins at the apical membrane that are dependent on ERM-1 for trafficking to maintain the apical junction. DLG-1 has also been shown to have a role in trafficking.

Human DLG-1/SAP97 is involved in trafficking of ionotropic receptors from the endoplasmic reticulum to the plasma membrane (Sans *et al.*, 2001), and *Drosophila* DLG-1/Dlg is involved in polarized trafficking to form membranes (Lee *et al.*, 2003). Therefore disassociation of DLG-1 from membranes could affect its role at junctions and in trafficking. Finally, there is precedent for DLG-1 interacting with Arp2/3. DLG-1 and Arp2/3-dependent actin cooperate during T-cell activation according to several studies (Xavier *et al.*, 2004; Round *et al.*, 2005). Further studies of how these proteins interact at the apical junction and contribute to trafficking will be needed to clarify their roles in epithelial polarity maintenance.

MATERIALS AND METHODS

Strains

C. elegans strains were cultured as described in Brenner (1974). The following strains were used in this analysis: WM43 gex-3(zu196)/DnT1, OX232 wve-1(zu469) unc-101(m1)/hin1; WM58 unc-24 gex-3 (zu196); Ex[GFP::GEX-3], RT1120 vha-6::ph::gfp, FT48 xnIs16 [dlg-1::gfp]; him-8, OX306 Is20 [vha-6::rde-4::gfp], FT250 xnIs96 [pJN455: hmr-1p::hmr-1::gfp::unc-54 3′UTR; unc-119(+); unc-119 (ed3)], OX515 fgEx11 [erm-1::gfp, rol-6]; mcIs46 [dlg-1::RFP; unc-119+], OX322 gex-2(ok1630)/dpy-9; xnIs16 [dlg-1::gfp], OX323 gex-3(zu196)/Dnt1; xnIs16 [dlg-1::gfp], OX309 wve-1(zu469) unc-101(m1)/hin1; xnIs16 [dlg-1::gfp], NG0324 wsp-1(gm324) SU159 ajm-1(ok160) X; jcEX44, IK537 sax-7(nj48), CX2993 sax-7(ky146); kyIs4, RB1199 sax-7 (ok1244), JJ1068 hmp-2(zu364)/hIn1, SU251 hmp-1(zu278); jcEX72 (pRF4, hmp-1::gfp), VJ311 erm-1(tm677)/unc-63(x18) dpy-5(e61), DH1201 rme-1(b1045).

Lysates for biochemistry

Mixed lysates were homogenized in lysis buffer (150 mM NaCl, 25 mM HEPES, 1 mM EDTA, 0.1% Triton, and protease inhibitor cocktail [11836153001; Roche Diagnostics, Indianapolis, IN]) in a stainless steel homogenizer (357572; Wheaton Science Products, Millville, NJ). Lysates were spun at 5K for 5 min, and the supernatant fraction was flash frozen in liquid nitrogen for Western blots.

Subcellular fractionations

Lysates were prepared as described, with the exclusion of Triton X-100 from the lysis buffer, and were processed immediately. The lysate was spun at increasing speeds and times using an Optima TLX Ultracentrifuge (Beckman Coulter, Brea, CA), rotor TLA-120.2. After each spin, the supernatant was removed and spun at the next speed. The spin speeds and times were as follows: spin 1, 1000 × *g* for 10 min; spin 2,10,000 × *g* for 10 min; spin 3, 30,000 × *g* for 20 min; spin 4, 100,000 × *g* for 90 min. At each step the pellet was resuspended in the same volume as the starting supernatant for that fraction. Then 5× Laemmli buffer was added to each fraction, and the fractions were boiled at 95°C for 5 min before loading on gels for Western blotting. Equal volumes of each supernatant and pellet pair were loaded per lane.

Feeding RNAi

For all feeding RNAi experiments, cDNAs of the genes were inserted into L4440 vector and transformed into HT115 cells. Saturated overnight cultures were diluted 1:250 and grown for 6–7 h until the OD_{600} was close to 1. Bacteria were resuspended in lysogeny broth containing ampicillin (Amp), 100 µg/ml. Isopropyl β-D-1-thiogalactopyranoside, 1 mM, was added to the bacteria and Amp plates before use. *C. elegans* animals were synchronized by hypochlorite treatment followed by hatching in M9 buffer. For lysate preparation L1 worms were fed either control HT115 *Escherichia coli* or HT115 containing the L4440 plasmid carrying the gene of interest and were grown at 22°C for 3 d. Lysates were made from the mixed population of adults and eggs. For embryonic analysis, embryos were collected on day 3 and imaged. For adult analysis, animals were assayed for several intestinal phenotypes on day 3, except for animals fed *arp-2* dsRNA, which were assayed on both day 2 and day 3.

Live imaging of embryos

Two- to four-cell-stage embryos (0–20 min after first cleavage) were dissected from adult hermaphrodites and mounted either on a 3% agarose pads or with glass beads (Monodisperse Standards, 25.60 µm, MS0026; Whitehouse Scientific Chester, United Kingdom). The embryos were incubated at 22°C for 240 min and then imaged every 40 min for the next 200 min. The interval was chosen to reduce photobleaching of the signal and to avoid damage to the embryo due to the exposure to UV light. All images were acquired on an Axioskop 2 Plus microscope (Zeiss, Thornwood, NY) using a 40× oil objective with iVision 4.0 software driving a sensicam qe camera (Cooke, Romulus, MI) and analyzed using ImageJ software (National Institutes of Health, Bethesda, MD).

Immunostaining and microscopy of embryos

For visualizing apical intestinal actin in the embryos, embryos were attached to poly-L-lysine slides and permeabilized by freeze cracking after 15 min on dry ice. The slides were fixed in a 4% paraformaldehyde solution for 10 min at room temperature. Embryos were incubated in Alexa Fluor 488 phalloidin (Molecular Probes, Invitrogen, Carlsbad, CA) diluted to 6.6 µM in phosphate-buffered saline (PBS) at room temperature for 1 h. Slides were mounted in PGND solution (1× PBS containing 80% glycerol, 4% [wt/vol] antifade [*n*-propyl gallate], and 0.4 mM 4′,6-diamidino-2-phenylindole [DAPI]). For immunohistochemistry, embryos were affixed to polylysine slides and freeze cracked as described earlier. Slides were then fixed in methanol for 20 min at −20°C. Slides were blocked in 2% PBST for 5 min, washed three times with PBS, and incubated with primary antibodies for 1 h at 37°C. Slides were then washed three times with PBS and incubated with secondary fluorophore-conjugated antibodies for 1 h at 37°C. Slides were mounted in PGND solution as described. All images were acquired on a Zeiss Axioskop 2 Plus microscope using a 40× oil objective with iVision 4.0 software driving a Cooke sensicam qe camera. The images were then analyzed using ImageJ software.

Immunostaining and microscopy of adults

For phalloidin staining of adult intestines 30–40 gravid adults or L4 worms were placed in cutting buffer (5% sucrose, 100 mM NaCl, 0.02 mM levamisole) and were sliced behind the pharynx using two 26½-gauge needles. The extruded intestine was transferred using a capillary tube coated with Sigmacote (Sigma-Aldrich, St. Louis, MO) onto a polylysine slide. Tissues were fixed in 1.25% paraformaldehyde for 10 min at room temperature. The slides were washed four times within 30 min in PBT (1% bovine serum albumin [BSA], 1× PBS, 0.1% Tween 20, 0.05% NaN_3, 1 mM EDTA) and then incubated in BODIPY FL phalloidin (B607; Molecular Probes, Invitrogen) diluted in PBS to a final concentration of 6.6 µM and incubated for 1 h at room temperature. The slides were then washed in PTC (1% BSA, 1× PBS + 0.1% Tween 20, 0.05% NaN_3, 1 mM EDTA) with four buffer changes in 1 hr. The slides were mounted in PGND solution (1× PBS containing 80% glycerol, 4% [wt/vol] *n*-propyl gallate as antifade, and 0.4 mM DAPI). Images were acquired on a Zeiss Axioskop 2 Plus

microscope using a 40× oil objective with iVision 4 Software driving a Cooke sensicam qe camera. All of the images were analyzed and measured using ImageJ.

Quantitation of immunofluorescence

Quantitation of phalloidin staining was performed using ImageJ software, including the rectangular selection and mean measure tools to measure average fluorescence of equal areas at the apical region of the intestine. Quantitation of live fluorescence was performed using the line selection and the dynamic profile function of ImageJ to measure fluorescence along lines of equal length that transversed the apical intestine and the cytoplasmic regions of the intestinal cells. The center of the line was placed over the apical intestine, and the maximum reading generated from that region was recorded as the apical signal. The cytoplasmic signal was calculated as the average of the signal at the center of the two intestinal cells 2.5 µm on either side of the apical intestine. For all of the experiments shown, the images were captured at the same exposure settings for wild type and mutants. Grouped images in each figure were assembled using the Mosaic function of iVision. All quantitation was done on the raw images. The figure legends indicate when images were enhanced for contrast, and the same enhancement was applied to a mosaic of the related images for that experiment.

Electron microscopy

Synchronized L1s were plated on control food or on RNAi food for 3 d. On the third day, the embryos were collected with sodium hypochlorite treatment. A total of 50 µl of packed embryos was transferred to an Eppendorf tube and incubated at room temperature with agitation for 10 min in 1×10^{-3} unit chitinase (C7809; Sigma-Aldrich) made in embryonic buffer (120 mM NaCl, 40 mM KCl, 3 mM $CaCl_2$, 3 mM $MgCl_2$, 5 mM HEPES, pH 7.2). Embryos were washed three times for 10 min each in 1 ml of M9 buffer. The samples were fixed for 2 d at 4°C in fresh 4% paraformaldehyde (15710; Electron Microscopy Sciences, Hatfield, PA) and 2% glutaraldehyde (16220; Electron Microscopy Sciences) in embryonic buffer. On the third day, the embryos were washed three times for 10 min in 1 ml of M9. M9 was replaced with 1% OsO4 for a 1-h incubation. Samples were dehydrated on a nutator at room temperature for 10 min sequentially with 50% ethanol, 70% ethanol, 95% ethanol, and 100% ethanol and twice with 100% acetone. The samples were then incubated in a series of graded Epon/acetone solutions. Epon/acetone (1:1) solution was used at room temperature for 2 h, followed by (3:1) Epon/acetone incubation overnight at room temperature on a nutator. The solution was replaced with 100% resin and microwaved in a Pelco microwave (Ted Pella, Redding, CA) at 250 W with the vacuum on for 3 min. The microwave cycle was repeated with new 100% resin, and the vacuum was left on for an additional 30 min. The resin was then replaced with clean 100% resin, spun, and baked at 70°C overnight. For all buffer changes, spins were performed at 3000 rpm for 3 min. The samples were separated from the Eppendorf tube, and 80- to 90-nm thin sections were cut using a Diatome diamond knife. The sections were picked up on 200-mesh, thin-bar copper grids and stained with uranyl acetate and lead citrate. Samples were imaged using an Advanced Microscopy Techniques (Woburn, MA) camera on a Philips (Briarcliff Manor, NY) CM12 electron microscope.

Statistical analysis

All graphs show the mean of the data and the standard error of the mean (SEM). For grouped data, statistical significance was established by performing a two-way analysis of variance (ANOVA), followed by the Bonferroni multiple comparisons posttest. For ungrouped data, a one-way ANOVA was performed followed by the Tukey posttest. Asterisks denote $p < 0.05$. All statistical analysis was performed using GraphPad Prism (GraphPad Software, La Jolla, CA).

ACKNOWLEDGMENTS

We thank the National Center for Research Resources–funded *Caenorhabditis* Genetics Center, Jeff Hardin, Alison Lynch, Barth Grant, Jeremy Nance, Verena Göbel, and Christopher Rongo for strains; Giorgio Scita for the EPS-8 antibodies; the National Institute of Child Health and Human Development–funded University of Iowa Hybridoma Bank for the MH27, ERM-1, SQV-8, DLG-1, and HMR-1 antibodies; Rajesh Patel and David Hall for help with the TEM; and Ramsey Foty for advice on statistics. We thank our colleagues for helpful suggestions on the manuscript: Andy Singson, William Wadsworth, Loren Runnels, Matthew Buechner, and two particularly helpful anonymous reviewers. Y.Y.B. received a Graduate Assistance in Areas of National Need predoctoral fellowship. This research was funded by grants from the National Institutes of Health (GM081670) and National Science Foundation (0641123) to M.C.S.

REFERENCES

Allen RD, Wolf RW (1979). Membrane recycling at the cytoproct of *Tetrahymena*. J Cell Sci 35, 217–227.

Audhya A, Desai A, Oegema K (2007). A role for Rab5 in structuring the endoplasmic reticulum. J Cell Biol 178, 43–56.

Bae YK, Kim E, L'Hernault SW, Barr MM (2009). The CIL-1 PI 5-phosphatase localizes TRP polycystins to cilia and activates sperm in *C. elegans*. Curr Biol 19, 1599–1607.

Benjamin JM, Kwiatkowski AV, Yang C, Korobova F, Pokutta S, Svitkina T, Weis WI, Nelson WJ (2010). Alpha E-catenin regulates actin dynamics independently of cadherin-mediated cell-cell adhesion. J Cell Biol 189, 339–352.

Bossinger O, Klebes A, Segbert C, Theres C, Knust E (2001). Zonula adherens formation in *Caenorhabditis elegans* requires *dlg-1*, the homologue of the *Drosophila* gene *discs large*. Dev Biol 230, 29–42.

Brenner S (1974). The genetics of *Caenorhabditis elegans*. Genetics 77, 171–94.

Chhabra ES, Higgs HN (2007). The many faces of actin: matching assembly factors with cellular structures. Nat Cell Biol 9, 1110–1121.

Chen CC, Schweinsberg PJ, Vashist S, Mareiniss DP, Lambie EJ, Grant BD (2006). RAB-10 is required for endocytic recycling in the *Caenorhabditis elegans* intestine. Mol Biol Cell 17, 1286–1297.

Chen L, Ong B, Bennett V (2001). LAD-1, the *Caenorhabditis elegans* L1CAM homologue, participates in embryonic and gonadal morphogenesis and is a substrate for fibroblast growth factor receptor pathway-dependent phosphotyrosine-based signaling. J Cell Biol 154, 841–855.

Cheshire AM, Kerman BE, Zipfel WR, Spector AA, Andrew DJ (2008). Kinetic and mechanical analysis of live tube morphogenesis. Dev Dyn 237, 2874–2888.

Chirivino D, Del Maestro L, Formstecher E, Hupe P, Raposo G, Louvard D, Arpin M (2011). The ERM proteins interact with the HOPS complex to regulate the maturation of endosomes. Mol Bio Cell 22, 375–385.

Costa M, Raich W, Agbunag C, Leung B, Hardin J, Priess JR (1998). A putative catenin-cadherin system mediates morphogenesis of the *Caenorhabditis elegans* embryo. J Cell Biol 141, 297–308.

Croce A, Cassata G, Disanza A, Gagliani MC, Tacchetti C, Malabarba MG, Carlier MF, Scita G, Baumeister R, Di Fiore PP (2004). A novel actin barbed-end-capping activity in EPS-8 regulates apical morphogenesis in intestinal cells of *Caenorhabditis elegans*. Nat Cell Biol 6, 1173–1179.

Ding M, King RS, Berry EC, Wang Y, Hardin J, Chisholm AD (2008). The cell signaling adaptor protein EPS-8 is essential for C. elegans epidermal elongation and interacts with the ankyrin repeat protein VAB-19. PLoS One 3, e3346.

Drees F, Pokutta S, Yamada S, Nelson WJ, Weis WI (2005). α-Catenin is a molecular switch that binds E-cadherin–β-catenin and regulates actin-filament assembly. Cell 123, 903–915.

Farah CA, Liazoghli D, Perreault S, Desjardins M, Guimont A, Anton A, Lauzon M, Kreibich G, Paiement J, Leclerc N (2005). Interaction of

microtubule-associated protein-2 and p63: a new link between microtubules and rough endoplasmic reticulum membranes in neurons. J Biol Chem 280, 9439–9449.
Fehon RG, McClatchey AI, Bretscher A (2010). Organizing the cell cortex: the role of ERM proteins. Nat Rev Mol Cell Biol 11, 276–287.
Firestein BL, Rongo C (2001). DLG-1 is a MAGUK similar to SAP97 and is required for adherens junction formation. Mol Biol Cell 12, 3465–3475.
Francis R, Waterston RH (1991). Muscle cell attachment in *Caenorhabditis elegans*. J Cell Biol 114, 465–479.
Fricke R, Gohl C, Dharmalingam E, Grevelhorsten A, Zahedi B, Harden N, Kessels M, Qualmann B, Bogdan S (2009). *Drosophila* Cip4/Toca-1 integrates membrane trafficking and actin dynamics through WASP and SACR/WAVE. Curr Biol 19, 1429–1437.
Georgiou M, Marinari E, Burden J, Baum B (2008). Cdc42, Par6, and aPKC regulate Arp2/3-mediated endocytosis to control local adherens junction stability. Curr Biol 18, 1631–1638.
Giuliani C *et al*. (2009). Requirements for F-BAR proteins TOCA-1 and TOCA-2 in actin dynamics and membrane trafficking during *Caenorhabditis elegans* oocyte growth and embryonic epidermal morphogenesis. PLoS Genet 5, e1000675.
Göbel V, Barrett PL, Hall DH, Fleming JT (2004). Lumen morphogenesis in *C. elegans* requires the membrane-cytoskeleton linker erm-1. Dev Cell 6, 865–873.
Grana TM *et al*. (2010). SAX-7/L1CAM and HMR-1/cadherin function redundantly in blastomere compaction and nonmuscle myosin accumulation during *Caenorhabditis elegans* gastrulation. Dev Biol 344, 731–744.
Grant B, Hirsh D (1999). Receptor-mediated endocytosis in the *Caenorhabditis elegans* oocyte. Mol Biol Cell 10, 4311–4326.
Grant B, Zhang Y, Paupard MC, Lin SX, Hall DH, Hirsh D (2001). Evidence that RME-1, a conserved *C. elegans* EH-domain protein, functions in endocytic recycling. Nat Cell Biol 3, 573–579.
Hadwiger G, Dour S, Arur S, Fox P, Nonet ML (2010). A monoclonal antibody toolkit for *C. elegans*. PLoS One 5, e10161.
Koppen M, Simske JS, Sims PA, Firestein BL, Hall DH, Radice AD, Rongo C, Hardin JD (2001). Cooperative regulation of AJM-1 controls junctional integrity in *Caenorhabditis elegans* epithelia. Nat Cell Biol 3, 983–991.
Kunda P, Pelling AE, Liu T, Baum B (2008). Moesin controls cortical rigidity, cell rounding, and spindle morphogenesis during mitosis. Curr Biol 18, 91–101.
Labouesse M (2006). Epithelial junctions and attachments. WormBook 13, 1–21.
Lee OK, Frese KK, James JS, Chadda D, Chen ZH, Javier RT, Cho KO (2003). Discs-Large and Strabismus are functionally linked to plasma membrane formation. Nat Cell Biol 5, 987–993.
Leibfried A, Fricke R, Morgan MJ, Bogdan S, Bellaiche Y (2008). *Drosophila* Cip4 and WASP define a branch of the Cdc42-Par6-aPKC pathway regulating E-cadherin endocytosis. Curr Biol 18, 1639–1648.
Leung B, Hermann GJ, Priess JR (1999). Organogenesis of the *Caenorhabditis elegans* intestine. Dev Biol 216, 114–134.
Manno S, Takakuwa Y, Mohandas N (2005). Modulation of erythrocyte membrane mechanical function by protein 4.1 phosphorylation. J Biol Chem 280, 7581–7587.
McMahon L, Legouis R, Vonesch JL, Labouesse M (2001). Assembly of *C. elegans* apical junctions involves positioning and compaction by LET-413 and protein aggregation by the MAGUK protein DLG-1. J Cell Sci 114, 2265–2277.
Nishikawa S, Kitamura H (1984). Cell membrane-associated microtubules in secretory ameloblasts of rat incisor. J Electron Microsc 33, 34–38.
Patel FP, Bernadskaya YY, Chen E, Jobanputra A, Pooladi Z, Freeman KL, Gally C, Mohler WA, Soto MC (2008). The WAVE/SCAR complex promotes polarized cell movements and actin enrichment in epithelia during *C. elegans* embryogenesis. Dev Biol 324, 297–309.
Raich WB, Agbunag C, Hardin J (1999). Rapid epithelial-sheet sealing in the *Caenorhabditis elegans* embryo requires cadherin-dependent filopodial priming. Curr Biol 9, 1139–1146.
Round JL, Tomassian T, Zhang M, Patel V, Schoenberger SP, Miceli MC (2005). Dlgh1 coordinates actin polymerization, synaptic T cell receptor and lipid raft aggregation, and effector function in T cells. J Exp Med 201, 419–430.
Sans N, Racca C, Petralia RS, Wang YX, McCallum J, Wenthold RJ (2001). Synapse-associated protein 97 selectively associates with a subset of AMPA receptors early in their biosynthetic pathway. J Neurosci 21, 7506–7516.
Schafer DA, Mooseker MS, Cooper JA (1992). Localization of capping protein in chicken epithelial cells by immunofluorescence and biochemical fractionation. J Cell Biol 118, 335–346.
Segbert C, Johnson K, Theres C, van Fürden D, Bossinger O (2004). Molecular and functional analysis of apical junction formation in the gut epithelium of *Caenorhabditis elegans*. Dev Biol 266, 17–26.
Silva JM *et al*. (2009). Cyfip1 is a putative invasion suppressor in epithelial cancers. Cell 137, 1047–1061.
Smutny M, Yap AS (2010). Neighborly relations: cadherins and mechanotransduction. J Cell Biol. 189, 1107–1115.
Soto MC, Qadota H, Kasuya K, Inoue M, Tsuboi D, Mello CC, Kaibuchi K (2002). The GEX-2 and GEX-3 proteins are required for tissue morphogenesis and cell migrations in *C. elegans*. Genes Dev 16, 620–632.
Stauffer TP, Ahn S, Meyer T (1998). Receptor-induced transient reduction in plasma membrane PtdIns(4,5)P_2 concentration monitored in living cells. Curr Biol 8, 343–346.
Totong R, Achilleos A, Nance J (2007). PAR-6 is required for junction formation but not apicobasal polarization in *C. elegans* embryonic epithelial cells. Development 134, 1259–1268.
van Furden D, Johnson K, Segbert C, Bossinger O (2004). The *C. elegans* ezrin-radixin-moesin protein ERM-1 is necessary for apical junction remodelling and tubulogenesis in the intestine. Dev Biol 272, 262–276.
Varnai P, Balla T (1998). Visualization of phosphoinositides that bind pleckstrin homology domains: calcium- and agonist-induced dynamic changes and relationship to myo-[^{3}H]inositol-labeled phosphoinositide pools. J Cell Biol 143, 501–510.
Withee J, Galligan B, Hawkins N, Garriga G (2004). *Caenorhabditis elegans* WASP and Ena/VASP proteins play compensatory roles in morphogenesis and neuronal cell migration. Genetics 167, 1165–1176.
Xavier R *et al*. (2004). Discs large (Dlg1) complexes in lymphocyte activation. J Cell Biol 166, 173–178.
Yamada S, Nelson WJ (2007). Localized zones of Rho and Rac activities drive initiation and expansion of epithelial cell-cell adhesion. J Cell Biol 178, 517–527.
Yonemura S, Wada Y, Watanabe T, Nagafuchi A, Shibata M (2010). Alpha-catenin as a tension transducer that induces adherens junction development. Nat Cell Biol 12, 533–542.
Zallen JA, Cohen Y, Hudson AM, Cooley L, Wieschaus E, Schejter ED (2002). SCAR is a primary regulator of Arp2/3-dependent morphological events in *Drosophila*. J Cell Biol 156, 689–701.
Zanin MKB, Donohue JM, Everitt BA (2010). Evidence that core histone H3 is targeted to the mitochondria in *Brassica oleracea*. Cell Biol Int 34, 997–1003.